In vivo probe-based confocal laser endomicroscopy in amiodarone-related pneumonia

Mathieu Salaün[1,2], Francis Roussel[3], Geneviève Bourg-Heckly[4], Christine Vever-Bizet[4], Stéphane Dominique[1], Anne Genevois[5], Vincent Jounieaux[6], Gérard Zalcman[7], Emmanuel Bergot[7], Jean-Michel Vergnon[8] and Luc Thiberville[1,2]

Affiliations: [1]Clinique Pneumologique, Rouen University Hospital, Rouen, F-76031, [2]Laboratoire QuantIF-LITIS EA 4108, Rouen University, Rouen, [3]Dept of Pathology and Cytology, Rouen University Hospital, Rouen, [4]Laboratoire Acides Nucléiques et Biophotonique "ANBioPhy", CNRS FRE 3207, Paris 6 University, Evry, [5]Dept of Radiology, Rouen University Hospital, Rouen, F-76031, [6]Dept of Pneumology, Amiens University Hospital, Amiens, [7]Dept of Pneumology, Caen University Hospital, Caen, and [8]Dept of Pneumology and Thoracic Oncology, Saint-Etienne University Hospital, Saint-Etienne, France.

Correspondence: L. Thiberville, Clinique Pneumologique, Hôpital Charles Nicolle, CHU de Rouen, 1 rue de Germont, 76031 Rouen Cedex, France. E-mail: Luc.Thiberville@univ-rouen.fr

ABSTRACT Probe-based confocal laser endomicroscopy (pCLE) allows microscopic imaging of the alveoli during bronchoscopy. The objective of the study was to assess the diagnostic accuracy of pCLE for amiodarone-related pneumonia (AMR-IP).

Alveolar pCLE was performed in 36 nonsmoking patients, including 33 consecutive patients with acute or subacute interstitial lung disease (ILD), of which 17 were undergoing treatment with amiodarone, and three were amiodarone-treated patients without ILD.

Nine out of 17 patients were diagnosed with high-probability AMR-IP (HP-AMR-IP) by four experts, and three separate observers. Bronchoalveolar lavage findings did not differ between HP-AMR-IP and low-probability AMR-IP (LP-AMR-IP) patients. In HP-AMR-IP patients, pCLE showed large (>20 μm) and strongly fluorescent cells in 32 out of 38 alveolar areas. In contrast, these cells were observed in only two out of 39 areas from LP-AMR-IP patients, in one out of 59 areas from ILD patients not receiving amiodarone and in none of the 10 areas from amiodarone-treated patients without ILD ($p<0.001$; HP-AMR-IP *versus* other groups). The presence of at least one alveolar area with large and fluorescent cells had a sensitivity, specificity, negative predictive value and positive predictive value for the diagnosis of AMR-IP of 100%, 88%, 100% and 90%, respectively.

In conclusion, pCLE appears to be a valuable tool for the *in vivo* diagnosis of AMR-IP in subacute ILD patients.

@ERSpublications
Probe-based confocal laser endomicroscopy appears useful for diagnosis of amiodarone-related pneumonia in subacute ILD http://ow.ly/ongMj

Received: Nov 03 2011 | Accepted after revision: Sept 17 2012 | First published online: Sept 27 2012

Clinical trial: This study is registered at clinicaltrials.gov with identifier number NCT00213603.

Support statement: This study was supported by the French Canceropole Nord-Ouest (Lille, France), the French Ministry of Health (PHRC 2007, Paris, France) and ADIR Association (Rouen, France).

Conflict of interest: Disclosures can be found alongside the online version of this article at www.erj.ersjournals.com

Introduction

Amiodarone, a class III anti-arrhythmic agent, is one of the most commonly prescribed drugs worldwide [1]. Since its introduction in clinical practice, several serious adverse effects have been attributed to chronic amiodarone administration and have triggered major concerns [2]. The most severe amiodarone-related side-effect is pulmonary toxicity [3, 4], which may lead to life-threatening conditions, such as pulmonary fibrosis and acute respiratory distress syndrome [5–9]. The risk of amiodarone-related pneumonia (AMR-IP) has been estimated to be 1.0% per year [10–12]. Clinical data, laboratory tests, as well as radiological features of amiodarone-induced pulmonary toxicity on chest computed tomography (CT) scans, are usually not specific. Bronchoalveolar lavage (BAL) fluid microscopic examination may be helpful to exclude other aetiologies of interstitial lung diseases (ILDs) [13]. It usually discloses the presence of phospholipid-filled macrophages as well as increased counts of leukocytes and lymphocytes. It is generally accepted that the absence of foamy macrophages eliminates amiodarone toxicity, while their presence only confirms exposure to amiodarone [14]. As lung biopsy may be harmful in patients harbouring respiratory failure and cardiac disorders, the suspicion of AMR-IP usually leads to discontinuation of the drug, without having definite evidence of the drug's responsibility. Therefore, more reliable diagnostic criteria of AMR-IP are needed.

Probe-based confocal laser endomicroscopy (pCLE) is a new minimally invasive technique that makes it possible to provide microscopic imaging of a living tissue. The procedure enables the exploration of proximal bronchus and alveolar regions during bronchoscopy in real time [15–18]. Studies have demonstrated that the main endogenous fluorophore, observed with pCLE at 488 nm excitation wavelength, is the elastin, which is a major component of the distal lung interstitial network, present in the axial backbone of the alveolar ducts and alveolar entrances [19, 20]. Due to tobacco tar specific fluorescence, the technique also allows the imaging of alveolar macrophages in active smokers, while these cells are not visible in nonsmoking healthy subjects [16]. Therefore, the pCLE pulmonary semiology dramatically differs in smokers and nonsmokers and should be analysed separately [21].

The objective of this study was to determine the diagnostic accuracy of alveolar pCLE in amiodarone-induced lung toxicity. For this purpose, we analysed pCLE imaging data from nonsmoking patients presenting with subacute ILD and compared results between amiodarone-related pneumonia and other ILD patients.

Methods

Study design

In order to assess the diagnostic accuracy of pCLE for amiodarone-induced lung disease, all consecutive subjects recruited into the ALVEOLE trial (ClinicalTrials.gov identifier: NCT00213603) presenting with acute or subacute ILD were selected for the present study, whether or not they were under chronic amiodarone therapy. In addition, all amiodarone-treated patients without ILD recruited in the ALVEOLE trial were also selected.

In each case, the aetiological diagnosis of ILD was assessed by a panel of experts on the basis of clinical, radiological, biological and follow-up data. In addition to the panel's diagnosis, the amiodarone-treated patients group was subjected to a second review by three independent specialists without knowledge of the panel's conclusions. All of the reviews were performed blinded to pCLE data.

Two groups of subjects were defined according to the experts' reviews, as follows. 1) Group A consisted of all the patients undergoing amiodarone therapy, with three subgroups: group A1, comprising patients with interstitial pneumonia and high probability of amiodarone-related pneumonia (HP-AMR-IP); group A2, patients with interstitial or alveolar pneumonia and low probability of amiodarone-related pneumonia (LP-AMR-IP); and group A3, patients undergoing amiodarone therapy but without interstitial pneumonia. 2) Group B consisted of ILD patients who were not receiving amiodarone therapy. pCLE data from group A1 were compared to those from groups A2 and B.

Subjects

Patients were part of the cohort prospectively enrolled in the ALVEOLE trial from April 2006 to May 2011. The ALVEOLE trial was approved by the institution review board (No. CPP NO1: 2005/029, Rouen University Hospital, Rouen, France). All of the patients signed a written informed consent before the pCLE procedure.

Inclusion criteria in the ALVEOLE trial were: diffuse or focal parenchymal lung disease with indication for bronchoscopy, age >18 years, signed written informed consent. Exclusion criteria were: bleeding disorder, pulmonary hypertension, contraindication for a bronchoscopy, history of anatomical or functional pneumonectomy.

Patients included in the ALVEOLE trial were considered for the present study when the following criteria were present: nonsmoker or smoking cessation at least 6 months previous, subacute ILD (<3 months), non-ILD under amiodarone treatment.

Diagnosis of ILD

In order to establish the final aetiological diagnosis of ILD, patient's baseline clinical, radiological and biological data, as well as follow-up data, were analysed by a panel of four experts, including pulmonologists (G. Zalcman and V. Jounieaux), a radiologist (A. Genevois) and a pathologist (F. Roussel), blinded to the pCLE results. The diagnosis of AMR-IP was achieved based on the aforementioned information and, specifically, on the patient's evolution after drug discontinuation with or without corticosteroids treatment, and exclusion of other causes of interstitial lung disease.

For amiodarone-treated patients, a second assessment was performed separately by three independent specialists (L. Thiberville, S. Dominique and E. Bergot) 4 months after the panel's review, blinded to the pCLE results. This assessment was based on the same baseline and follow-up information, without knowledge of the conclusions of the previous panel. For this purpose, each expert rated patient's diagnosis as low, intermediate or high probability of AMR-IP. After both reviews, patients were classified as HP-AMR-IP when both the panel and at least two of the independent reviewers agreed.

In vivo, *real time alveolar microscopic imaging*

The pCLE imaging of alveolar areas was achieved using a Cellvizio Lung device with 488 nm excitation, coupled to a spectrometer (Mauna Kea Technologies, Paris, France). All of the endoscopic procedures were performed according to a protocol previously described [16]. Briefly, a 4.4-mm bronchoscope (MP60 model; Olympus, Tokyo, Japan) was inserted into the airways down to the smallest reachable bronchi. The pCLE miniprobe was then introduced into the working channel of the bronchoscope, and was pushed smoothly beyond the bronchoscope view into the successive divisions of the bronchial tree until it penetrated into a pulmonary lobule, as previously described [15–17, 22].

pCLE sequences were recorded and stored for subsequent analysis. As much as possible, pCLE alveolar imaging was performed in the regions of interest according to the chest CT scan abnormalities.

In situ *fluorescence microspectrometry*

Spectra of the microscopic area were recorded *in vivo* through the spectroscopic channel of the pCLE device, simultaneously with the image acquisition as previously described [16]. The spectral analysis was performed using a specific deconvolution (Levenbergt–Marquardt) algorithm. This algorithm is based on a linear combination of three spectral components: the normalised elastin and the tobacco tar emission spectra experimentally measured, and a Gaussian spectrum with tunable width and central wavelength. Spectra from AMR-IP patients were compared to those acquired in a previous study from smoking healthy volunteers [16].

Imaging data analysis

The pCLE image analysis was performed simultaneously by two observers (M. Salaün and L. Thiberville) blinded to the patient's charts and diagnosis.

Measurements were performed using the dedicated Medviewer® 1.1 software (Mauna Kea Technologies). Cell size was assessed according to its greatest dimension. Fluorescence intensity was quantified using the MedViewer Signal Quantification Toolbox, with the lower and upper level thresholds of the look-up table set to one and 8000, respectively. The pCLE features considered for quantitative analysis were as follows. 1) The presence of fluorescent cells: this feature was defined as the presence of at least one detectable cell per area explored during pCLE; 2) the presence of cells >20 or >30 μm, defined as the presence of at least one cell with a diameter >20 or >30 μm per area explored; 3) the cellular organisation, assessed by the number of areas where the cells appeared aggregated or isolated as analysed from the dynamic video sequences; and 4) the fluorescence intensity of the pCLE signal: fluorescence intensities were computed from the frames displaying the maximal cellular density. Fluorescence intensity results were expressed as the median of the pixels intensity for each selected frame.

Two kinds of analysis were performed: 1) per area analysis, in which the features (*e.g.* "the number of alveolar areas showing cellular infiltration", or "the number of alveolar areas with cells $\geqslant$20 μm") are compared on the basis of their frequency in each group; and 2) per patient analysis, where the number of patients presenting the pCLE features are compared between groups. For this purpose, pCLE features were defined as "positive" for one patient when present in at least one of the explored areas.

DOI: 10.1183/09031936.00191911

Bronchoaveolar lavage analysis

BAL was performed using four aliquots of 50 mL saline. Cytological cellular analysis of the BAL fluid included total and differential cell count, presence and semi-quantification of foamy macrophages and Golde score. Foamy macrophages were identified on the basis of their cytoplasmic aspect after May–Grünwald–Giemsa coloration, where the cytoplasm is filled by rounded vacuoles optically empty on conventional optical microscopy. The Golde score was assessed as described [23]. Briefly, a total of 100 individual macrophages were scored after staining by Perl's Prussian blue method. Each cell was ranked for hemosiderin content by using the following scale: 0, no colour; 1, faint blue in one portion of the cytoplasm; 2, deep blue in a minor portion of the cell; 3, deep blue in most areas of the cytoplasm; and 4, deep blue throughout the cell.

Statistics

The frequencies of the pCLE features were compared between groups using Fisher's exact test. The median fluorescence intensities were compared using the Mann–Whitney test.

Sensitivity, specificity, positive predictive value and negative predictive value, as well as 95% confidence intervals, were computed to assess the diagnosis accuracy of pCLE for AMR-IP.

To take into account multiple comparisons, the p-values presented are corrected according to Bonferroni, ($p_B=1-(1-p)^{1/n}$ where p is the uncorrected value, p_B is the corrected value of p, and n is the number of comparisons).

Results

Subjects

Subjects on amiodarone therapy

The classification of the patients undergoing amiodarone treatment as HP-AMR-IP and LP-AMR-IP did not differ between the panel's review and the three independent specialists' review. There was a good agreement between the independent observers ($\kappa=0.61$; Fleiss kappa).

After the experts' reviews, nine patients were diagnosed with HP-AMR-IP in the absence of an alternative diagnosis (group A1), and eight patients were classified in group A2, with LP-AMR-IP (alternative diagnoses were subacute cardiac failure (n=2), infectious pneumonia (n=2), organising pneumonia (n=2),

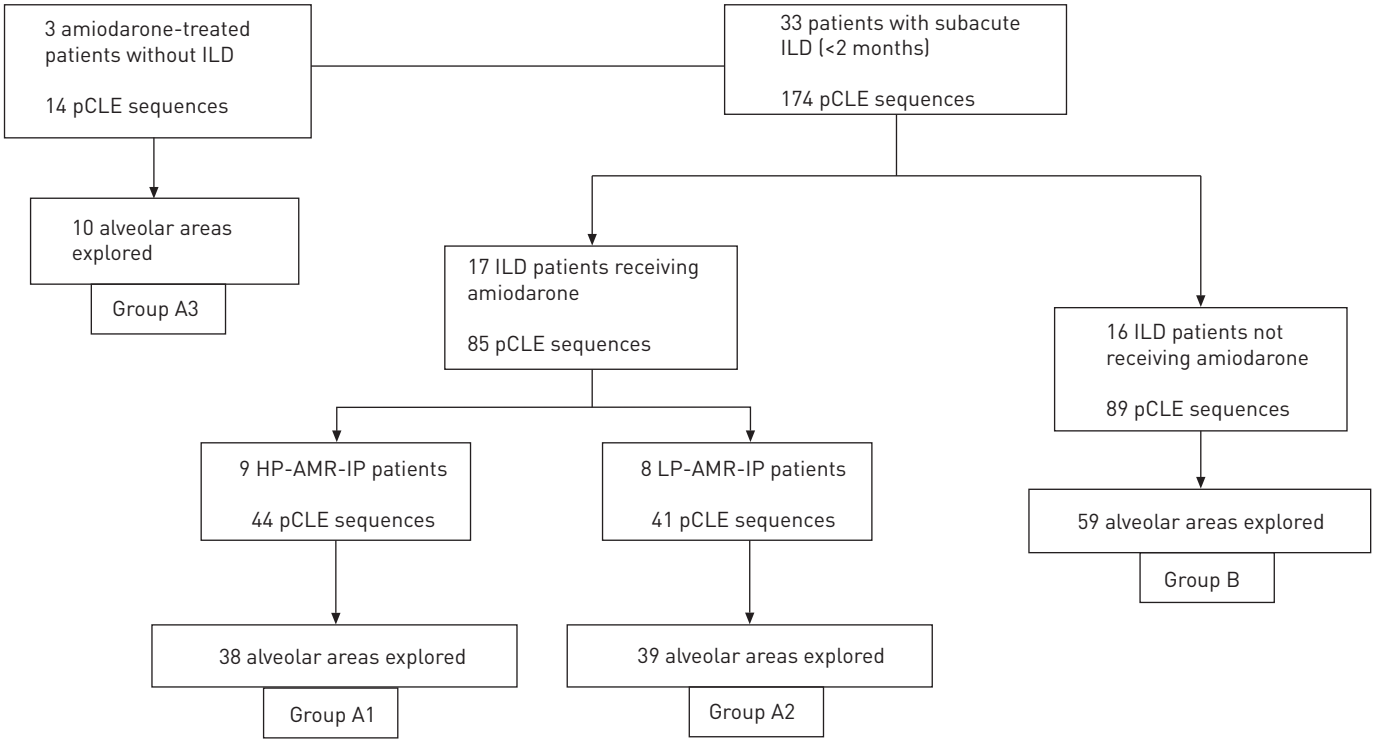

FIGURE 1 Flow chart of the subacute interstitial lung disease (ILD) patients undergoing the endomicroscopy procedure. pCLE: probe-based confocal laser endomicroscopy; HP-AMR-IP: high probability for amiodarone-related interstitial pneumonia; LP-AMR-IP: low probability for amiodarone-related interstitial pneumonia.

TABLE 1 Characteristics of the amiodarone-treated patients

Patient/age years/sex	Smoking status	Radio-clinical presentation	Chest CT scan	BAL results total cell count per mm^3/macrophages %/lymphocytes %	Amiodarone duration months/total dose g	Final diagnosis	Follow-up
Group A1							
1/79/F	Nonsmoker	Subacute diffuse interstitial pneumonia	GGO, alveolar septa thickening, consolidation	885/94/3	48/290	AMR-IP	Complete recovery after amiodarone cessation and corticosteroids treatment
2/77/F	Nonsmoker	Subacute diffuse interstitial pneumonia	GGO, alveolar septa thickening	790/39/52	72/430	AMR-IP	Complete recovery after amiodarone cessation and corticosteroids treatment
3/74/M	Ex-smoker	Subacute diffuse interstitial pneumonia	GGO, alveolar septa thickening	775/95/3	20/120	AMR-IP	Complete recovery of symptoms after amiodarone cessation
4/76/F	Nonsmoker	Subacute diffuse interstitial pneumonia	GGO, alveolar septa thickening	1500/69/22	13/78	AMR-IP	Progressive recovery after amiodarone cessation and corticosteroids treatment
5/69/M	Ex-smoker	Acute diffuse interstitial pneumonia Asbestos-related fibrosis	GGO, alveolar septa thickening, bronchiectasis, consolidation	1265/48/5	12/72	AMR-IP	Rapid improvement after amiodarone cessation and corticosteroids treatment
6/83/M	Nonsmoker	Subacute diffuse interstitial lung disease	GGO, alveolar septa thickening, consolidation, nodules	764/40/54	36/156	AMR-IP	Complete recovery after amiodarone cessation and corticosteroids treatment
7/84/M	Ex-smoker	Subacute diffuse interstitial lung disease	GGO, consolidation, pleural effusion	208/49/37	27/164	AMR-IP	Rapid improvement after amiodarone cessation and corticosteroids treatment
8/68/M	Ex-smoker	Subacute diffuse interstitial lung disease	GGO, consolidation	250/91/8	1/6	AMR-IP	Progressive recovery after amiodarone cessation and corticosteroids treatment
9/72/F	Nonsmoker	Acute diffuse interstitial lung disease	GGO, alveolar septa thickening, consolidation	590/26/36	10/60	AMR-IP	Death despite amiodarone cessation, corticosteroids and appropriate treatments in ICU
Group A2							
10/68/M	Ex-smoker	Subacute diffuse interstitial pneumonia	GGO, alveolar septa thickening	620/93/5	36/220	Acute cardiac failure	Rapid improvement after amiodarone cessation and treatment with antibiotics and diuretics.
11/88/F	Nonsmoker	Febrile subacute dyspnoea	Bilateral GGO and right upper lobe consolidation	NA	8/50	Infectious pneumonia associated with acute cardiac failure	Rapid improvement after amiodarone cessation and treatment with antibiotics and diuretics.
12/68/M	Ex-smoker	Subacute interstitial pneumonia	Asymmetric GGO	380/91/9	6/36	Infectious pneumonia	Complete recovery after amiodarone cessation and antibiotics
13/80/M	Nonsmoker	Febrile subacute dyspnoea and bilateral consolidation	Bilateral consolidation	180/54/23	60/360	Organising pneumonia	Progressive recovery after amiodarone cessation and corticosteroids treatment
14/84/F	Nonsmoker	Subacute interstitial pneumonia	GGO and consolidation	1180/95/3	13/78	Organising pneumonia	Progressive recovery after amiodarone cessation and corticosteroids treatment
15/82/M	Ex-smoker	Subacute interstitial pneumonia	Alveolar septa thickening, traction bronchiectasis	480/28/18	36/220	Asbestosis	Stable after amiodarone discontinuation
16/79/M	Ex-smoker	Subacute febrile interstitial pneumonia and weight loss	Consolidation, alveolar septa thickening, traction bronchiectasis	324/46/35	2/12	Allergic bronchopulmonary aspergillosis	Complete recovery after amiodarone cessation, corticosteroids, and itraconazole
17/87/F	Nonsmoker	Subacute febrile interstitial pneumonia	GGO	655/78/13	45/270	Acute cardiac failure/ chronic lymphoid leukaemia	Partial recovery after amiodarone cessation, corticosteroids, and diuretics
Group A3							
18/70/M	Ex-smoker	Peripheral lung nodule without interstitial pneumonia	Peripheral lung nodule	NA	72/440	Lung cancer	Death from lung cancer
19/76/M	Ex-smoker	Pulmonary emphysema and right upper lobe radio-occult carcinoma	Pulmonary emphysema	NA	17/102	Lung cancer	Ongoing treatment for lung cancer
20/70/M	Nonsmoker	Febrile subacute dyspnoea	Bronchiectasis and consolidation	NA	12/72	Infective exacerbation of bronchiectasis	Complete recovery after treatment with antibiotics

CT: computed tomography; BAL: bronchoalveolar lavage; F: female; M: male; GGO: ground-glass opacity; AMR-IP: amiodarone-related pneumonia; ICU: intensive care unit; NA: not available.

DOI: 10.1183/09031936.00191911

asbestosis (n=1) and allergic bronchopulmonary aspergillosis (n=1)). Three patients receiving amiodarone therapy had no interstitial lung disease (peripheral lung cancer, n=2; bronchiectasis, n=1) (group A3) (fig. 1).

The main characteristics of the patients under amiodarone therapy are indicated in table 1.

Among these subjects, 38 *in vivo* alveolar pCLE sequences were recorded from different lung segments in HP-AMR-IP patients (group A1), 39 alveolar sequences were recorded from group A2 patients (LP-AMR-IP), and 10 alveolar sequences were recorded from patients without ILDs (group A3) (fig. 1).

Subjects not receiving amiodarone therapy

16 patients with ILD without amiodarone therapy were diagnosed with hypersensitivity pneumonia (n=6, 23 alveolar areas explored), cryptogenic organising pneumonia (n=4, 17 alveolar areas), bleomycin-induced diffuse lung disease (n=2, five alveolar areas), autoimmune systemic disease (n=2, nine alveolar areas), eosinophilic lung (n=1, three alveolar areas), and *Pneumocystis jiroveci* pneumonia (n=1, two alveolar areas) (fig. 1).

In vivo *pCLE imaging*

The pCLE added a median (interquartile range) 7 (4–13) min to the whole endoscopic procedure. No serious adverse event, such as bleeding, post-bronchoscopy infection or pneumothorax occurred during the endomicroscopic procedures.

Alveolar cellular imaging and BAL data

Figure 2 shows the fluorescent signal from alveolar cells in amiodarone treated patients with and without HP-AMR-IP.

A characteristic infiltration of the alveoli with strongly fluorescent cells was present in all of the HP-AMR-IP patients, in 35 of the 38 acinar areas explored. The presence of large alveolar cells (>20 µm) with fluorescence >100 arbitrary units were observed in every patient with HP-AMR-IP and in 32 out of 38 areas explored from this group. These cells were detected in only one patient from group A2 (two out of 39 alveolar areas), as well as in another patient from group B (one of 59 alveolar areas). The presence of these highly fluorescent cells in at least one alveolar area could discriminate HP-AMR-IP from other ILD patients with a sensitivity of 100% (95% CI 0.66–1), specificity 88% (95% CI 0.47–1), and positive and negative predictive values of 90% (95% CI 0.55–1) and 100% (95% CI 0.59–0.1), respectively (tables 2 and 3).

In contrast, a faint cellular fluorescence was observed in six patients of group A2 and in one out of the three patients in group A3, in 14 out of 39 and two out of 10 alveolar areas explored, respectively (p<0.001, A1

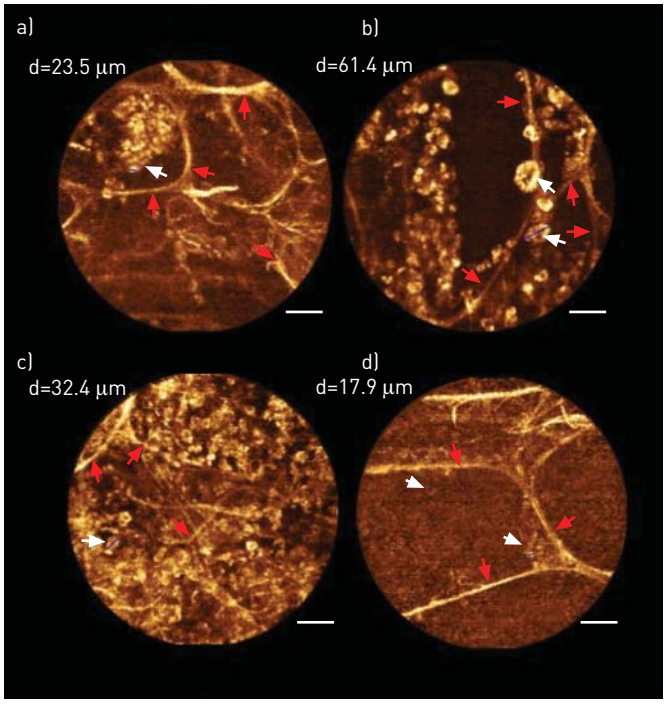

FIGURE 2 *In vivo* probe-based confocal laser endomicroscopy imaging in subacute interstitial lung disease patients undergoing amiodarone treatment. a–c) Specific infiltration of the alveolar spaces with large and highly fluorescent cells (white arrows) in amiodarone-related pneumonia patients. Red arrows indicate the elastic network that appears normal (a, b) or disorganised and dense (c). d) Mild alveolar cellular infiltration observed in a patient under amiodarone therapy, who was diagnosed with an acute cardiac failure associated with infectious pneumonia. The cells appeared smaller (<20 µm) and displayed a faint fluorescent signal (white arrows), in a normal acinar elastic network (red arrows). Images were retrieved from video sequences. An example of video is available in the online supplementary material. d: cell diameter. Scale bars= 50 µm.

TABLE 2 Per-area analysis of the probe-based confocal laser endomicroscopy (pCLE) cellular features in amiodarone-related pneumonia and in other interstital lung disease (ILD) patients

pCLE features	A1: HP-AMR-IP[#]	A2: LP-AMR-IP[¶]	B: ILD without amiodarone therapy[+]	p-value	Diagnostic accuracy of pCLE features for HP-AMR-IP[§] (95% CI)			
					Sensitivity	Specificity	PPV	NPV
Alveolar areas showing cellular infiltration	35	14	14	A1 *versus* A2 p<0.001[##] A1 *versus* B p<0.001[##] A2 *versus* B p=0.58	0.92 (0.79–0.98)	0.64 (0.47–0.79)	0.71 (0.57–0.83)	0.89 (0.72–0.98)
Alveolar areas with cells ⩾20 μm[f]	33	5	1	A1 *versus* A2 p<0.001[##] A1 *versus* B p<0.001[##] A2 *versus* B p=0.42	0.94 (0.81–0.99)	0.64 (0.35–0.87)	0.87 (0.72–0.96)	0.82 (0.48–0.98)
Alveolar areas with cells >30 μm[f]	25	3	0	A1 *versus* A2 p=0.009[##] A1 *versus* B p<0.001[##] A2 *versus* B p=0.30	0.71 (0.54–0.85)	0.79 (0.49–0.95)	0.89 (0.72–0.98)	0.52 (0.30–0.74)
Alveolar areas where the cells appeared aggregated[f]	16	2	1	A1 *versus* A2 p=0.15 A1 *versus* B p=0.05 A2 *versus* B p=1	0.46 (0.29–0.63)	0.86 (0.57–0.98)	0.89 (0.65–0.99)	0.39 (0.22–0.58)
Fluorescence intensity of alveolar cells AU[f]	344 (155–451)	101 (75–202)	105 (82–157)	A1 *versus* A2 p=0.003[¶¶] A1 *versus* B p=0.001[¶¶] A2 *versus* B p=0.99	NA	NA	NA	NA
Alveolar areas with cells >20 μm and fluorescence intensity >100 AU	32	2	1	A1 *versus* A2 p<0.001[##] A1 *versus* B p<0.001[##] A2 *versus* B p=0.92	0.84 (0.69–0.94)	0.95 (0.83–0.99)	0.94 (0.80–0.99)	0.86 (0.72–0.95)

Data are presented as n or median (interquartile range), unless otherwise stated. HP-AMR-IP: high-probability of amiodarone-related interstitial pneumonia; LP-AMR-IP: low-probability of amiodarone-related interstitial pneumonia; pCLE: probe-based confocal laser endomicroscopy; PPV: positive predictive value; NPV: negative predictive value; AU: arbitrary units; NA: not applicable. [#]: 38 alveolar areas explored; [¶]: 39 alveolar areas explored; [+]: 59 alveolar areas explored; [§]: group A1, control group is A2; [f]: data from alveolar areas showing cellular infiltration; [##]: significant values by Fisher's exact test, the p-values presented are corrected to take into account multiple comparisons (Bonferroni correction); [¶¶]: significant values by Mann–Whitney test, the p-values presented are corrected (Bonferroni).

DOI: 10.1183/09031936.00191911

DOI: 10.1183/09031936.00191911

TABLE 3 Per-patient analysis of the probe-based confocal laser endomicroscopy (pCLE) cellular features

pCLE features	A1: HP-AMR-IP[#]	A2: LP-AMR-IP[¶]	B: ILD without amiodarone therapy[+]	p-value	Diagnostic accuracy of pCLE features for HP-AMR-IP[§] (95% CI)			
					Sensitivity	Specificity	PPV	NPV
Patients showing alveolar cellular infiltration	9	6	6	A1 *versus* A2=0.50 A1 *versus* B=0.008[##] A2 *versus* B=0.29	1 (0.66–1)	0.25 (0.03–0.65)	0.60 (0.32–0.84)	1 (0.16–1)
Patients with alveolar cells ⩾20 μm[f]	9	1	1	A1 *versus* A2=0.005[##] A1 *versus* B=0.005[##] A2 *versus* B=1	1 (0.66–1)	0.83 (0.36–1)	0.9 (0.55–1)	1 (0.48–1)
Patients with alveolar cells ⩾30 μm[f]	8	1	0	A1 *versus* A2=0.03[##] A1 *versus* B=0.004[##] A2 *versus* B=1	0.89 (0.52–1)	0.83 (0.36–1)	0.89 (0.52–1)	0.83 (0.36–1)
Patients with alveolar areas where the cells appeared aggregated[f]	7	2	1	A1 *versus* A2=0.35 A1 *versus* B=0.11 A2 *versus* B=1	0.78 (0.4–0.97)	0.67 (0.22–0.96)	0.78 (0.4–0.97)	0.67 (0.22–0.96)
Fluorescence intensity of alveolar cells[f]	347±174	202±158	114±44	A1 *versus* A2=0.37 A1 *versus* B=0.02[##] A2 *versus* B=0.77	NA	NA	NA	NA
Patients with alveolar cells >20 μm and fluorescence intensity >100 AU	9	1	1	A1 *versus* A2=0.001[##] A1 *versus* B<0.001[##] A2 *versus* B=1	1 (0.66–1)	0.88 (0.47–1)	0.9 (0.55–1)	1 (0.59–1)

Data are presented as n or mean±SD, unless otherwise stated. HP-AMR-IP: high probability of amiodarone-related interstitial pneumonia; LP-AMR-IP: low probability of amiodarone-related interstitial pneumonia; ILD: interstitial lung disease; PPV: positive predictive value; NPV: negative predictive value; NA: not applicable. [#]: n=9; [¶]: n=8; [+]: n=16; [§]: group A1, control group is A2; [f]: cellular characteristics are quantified from patients with at least one area showing cellular infiltration; [##]: significant values by Fisher's exact test, the p-values presented here are corrected (Bonferroni).

versus A2 and A1 *versus* A3; Fisher's exact test) (table 2). Analysis of pCLE imaging in ILD patients without amiodarone medication (group B) also showed a faint cellular infiltration in only six out of 16 patients, in 14 out of the 59 alveolar areas explored (table 2).

Details of the pCLE cellular features are given in table 2 and figure 3. Alveolar cells from HP-AMR-IP patients (group A1) differed from the other groups by a larger size ($p<0.001$) and stronger fluorescence ($p<0.001$). Alveolar cells were more often aggregated in group A1 compared to ILD patients without amiodarone treatment ($p=0.05$) (table 2).

Table 4 and figure 3 describe the cellular population predominant on BAL analysis in comparison to the alveolar cellular features observed with pCLE. From the nine HP-AMR-IP patients, five presented with a predominant lymphocyte alveolitis, two with a neutrophil alveolitis, and two with a predominant macrophage alveolitis. Interestingly, pCLE analysis of the lymphocyte and neutrophil alveolitis cases showed two populations of fluorescent cells (fig. 4). One was made of small round and homogenous cells (presumably activated lymphocytes and/or neutrophils) that could be observed in the small bronchi before reaching the alveolar areas (fig. 4a; and online supplementary video); the other was an inhomogeneous population of larger cells within the alveolar areas, which may correspond to activated alveolar macrophages (fig. 4b). In the two AMR-IP patients with macrophage alveolitis on BAL, pCLE displayed only this population of larger cells.

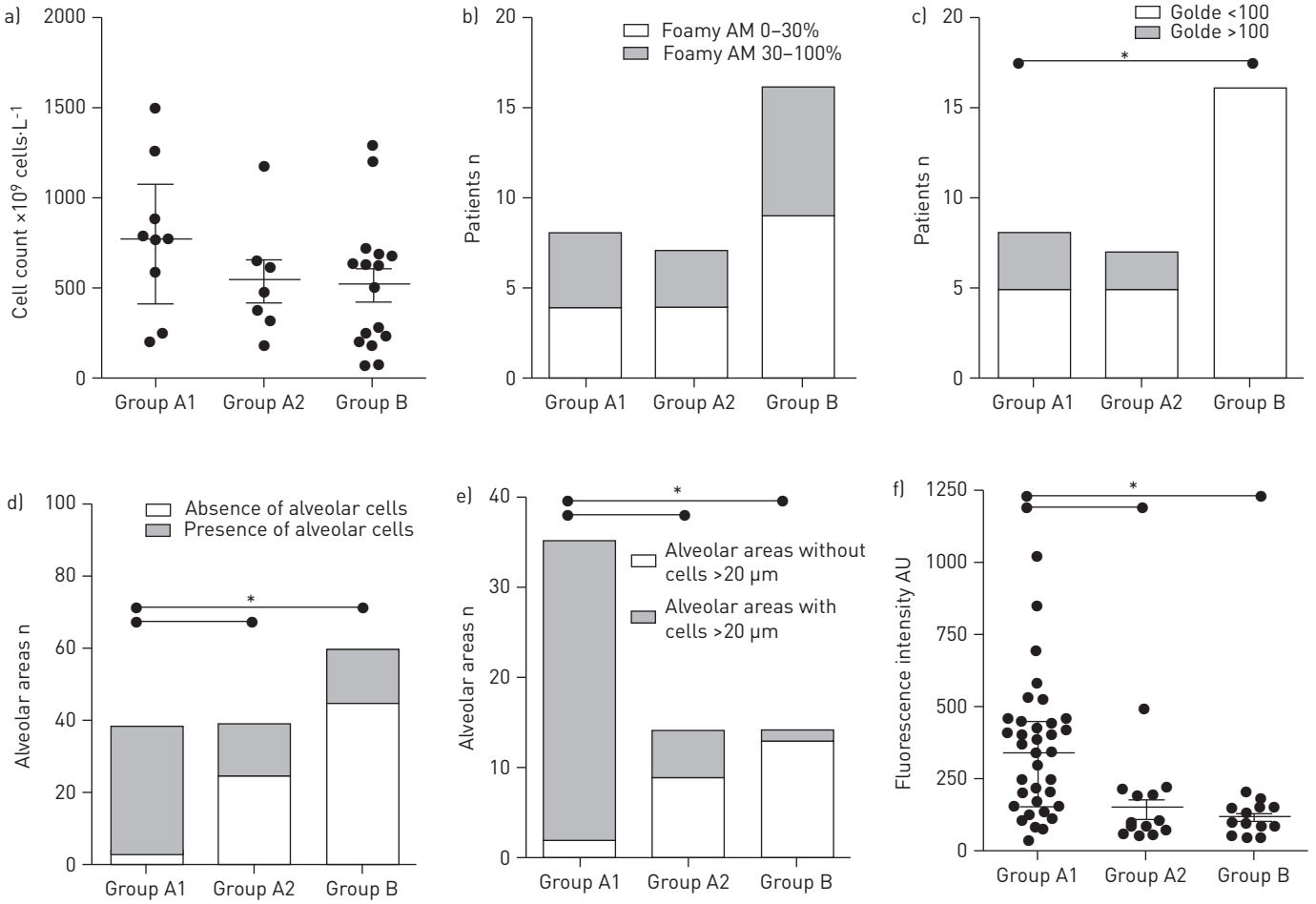

FIGURE 3 Comparison of bronchoalveolar lavage (BAL) and alveolar probe-based laser confocal endomicroscopy (pCLE) results. a) The total cellularity in BAL was not higher in the high probability amiodarone-related interstitial pneumonia (HP-AMR-IP) (medians with interquartile range) (Mann–Whitney test). b) The proportion of foamy alveolar macrophages (AMs) in BAL did not differ between groups (Fisher's exact test). c) The number of patients with Golde score >100 was higher in the HP-AMR-IP patients than in non-amiodarone treated patients with ILD, but did not differ between HP-AMR-IP and low probability for amiodarone-related interstitial pneumonia (LP-AMR-IP) patients. *: $p<0.05$, Fisher's exact test. d) The number of alveolar areas infiltrated with fluorescent cells observed with pCLE was significantly higher in HP-AMR-IP patients than in other groups. *: $p<0.05$, Fisher's exact test. e) The number of alveolar areas infiltrated with >20 µm fluorescent cells observed in pCLE was significantly higher in HP-AMR-IP patients than in other groups. *: $p<0.05$, Fisher's exact test. f) The cellular fluorescence intensity was higher in HP-AMR-IP patients than in the other groups (medians with interquartile range). *: $p<0.05$, Mann–Whitney test. AU: arbitrary units.

DOI: 10.1183/09031936.00191911

TABLE 4 Comparison of the cellular pattern from the bronchoalveolar lavage (BAL) fluid with probe-based confocal laser endomicroscopy (pCLE) findings in interstitial lung disease patients

Patients	BAL analysis						Size of alveolar cells observed *via* pCLE	
	Total cell count per mm^3	Type II alveolar cells[#]	AM %	Lymphocytes %	Foamy AM	Golde score	>20 μm	<20 μm
Group A1								
1	885	+	94	3	+++	175	Yes	No
2	790	-	39	52	+++	5	Yes	Yes
3	775	-	95	3	+++	360	Yes	No
4	1500	-	69	22	++	35	Yes	Yes
5	1265	-	48	5	+	0	Yes	Yes
6	764	-	40	54	+	1	Yes	Yes
7	208	-	49	37	+	0	Yes	Yes
8	250	NA	91	8	NA	NA	Yes	No
9	590	-	26	36	+	0	Yes	Yes
Group A2[¶]								
10	620	-	93	5	+	265	Yes	No
12	380	-	91	9	-	1	No	No
13	180	-	54	23	+++	0	No	Yes
14	1180	-	95	3	+++	0	No	No
15	480	-	28	18	+	0	No	Yes
16	324	-	46	35	++	0	No	Yes
17	655	-	78	13	+	180	No	Yes
Group B								
21	76	-	45	53	-	1	No	Yes
22	1200	-	40	57	+	16	No	Yes
23	1290	-	28	72	++	0	No	Yes
24	635	-	62	36	+	0	No	No
25	72	-	26	61	++	0	No	No
26	246	-	83	12	++	0	No	No
27	235	-	91	8	++	0	No	No
28	180	-	93	5	+	0	No	No
29	212	-	75	21	-	0	No	No
30	720	-	85	12	+	21	No	No
31	690	-	45	54	+	5	Yes	Yes
32	630	-	57	40	++	0	No	No
33	630	+	42	14	++	0	No	Yes
34	500	-	12	21	+	0	No	No
35	280	-	69	15	+++	0	No	No
36	675	-	56	44	+	1	No	Yes

AM: alveolar macrophage; NA: not available. +++: foamy macrophages/total AMs ratio in BAL is more than 75%; ++: foamy macrophages/total AMs ratio in BAL is 30–75%; +: foamy macrophages/total AMs ratio in BAL is less than 30%; -: no foamy macrophage. [#]: type II alveolar cells were absent (-), or were present and accounted in each case for less than 30% of the cellular population (+); [¶]: BAL data were not available from one patient with a mild cellular infiltration on pCLE imaging (patient 11) in group A2.

A morphology-based interpretation of the cell population is provided on the online supplementary material, suggesting that the large cell population may be activated macrophages. However, it cannot be excluded that some of the largest fluorescent cells on pCLE do represent alveolar type II cells (online supplementary material and fig. S1).

Foamy macrophages were not restricted to HP-AMR-IP but were also observed in the BAL of 20 other ILD patients. Semi-quantitative assessment of foamy macrophage number was not related to the presence of large fluorescent cells observed *in vivo* using pCLE (figure 3 and table 4).

Microspectrometry analysis

Results of microspectrometry analysis are indicated in figure 5. This analysis shows that HP-AMR-IP can be distinguished from LP-AMR-IP patients, as well as from smoking subjects on the basis of the autofluorescence spectra at 488 nm.

Further analysis showed that autofluorescence spectra at 488 nm from patients with HP-AMR-IP could be characterised by the combination of the reference spectrum of elastin and of another spectrum centred at 550 nm, which appears specific for amiodarone lung toxicity. As a comparison, the spectrum from smoking healthy volunteers could be modelled by the combination of three spectral components: the tobacco tar component and the elastin component, and a weak component centred at 630 nm (data not shown).

Discussion

This study indicates for the first time that pCLE is able to discriminate patients with amiodarone-related pneumonia from other ILDs. In the absence of validated diagnostic criteria of AMR-IP, these findings may have a significant clinical value.

Here, we found that a major pCLE characteristic of amiodarone-related pneumonia is the presence of highly fluorescent and large cells, presumably macrophages, within the alveoli. In our series, this item has positive and negative predictive values of 90% and 100%, respectively, for the diagnosis of AMR-IP. Besides its ability to diagnose AMR-IP among ILD patients receiving amiodarone, our study also suggests that pCLE can discriminate AMR-IP from other ILDs, including hypersensitivity pneumonia and other drug-induced pneumonia (furantoin- and bleomycin-induced fibrosis).

In AMR-IP patients, we were able to image these large fluorescent cells *in vivo* in 84% of the alveolar areas, including the patients with lymphocyte and/or neutrophil alveolitis. Interestingly, in these cases, the large fluorescent cells were observed along with smaller fluorescent cells, presumably lymphocyte or neutrophil populations, *in vivo*.

Our data demonstrate that the observation of fluorescent alveolar cells using pCLE has a better diagnostic value than BAL findings. Historically, foamy macrophages in BAL from patients with amiodarone lung toxicity have been observed since the early 1980s [13]. However, studies have demonstrated that these foamy cells can also be observed in patients under amiodarone therapy without ILD, suggesting that they represent more a marker of a routine drug effect than an indicator of lung toxicity [14]. Our findings

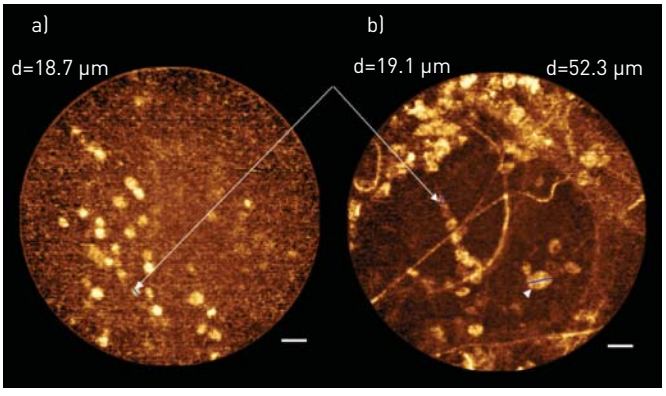

FIGURE 4 Examples of bronchiolar and alveolar cellular fluorescence in the same patient with high probability amiodarone-related pneumonia (patient 2). Two different fluorescent cellular populations are observed: a) regular, round cells in bronchioles (white arrow), and b) the association of small (white arrow) and large (white arrowhead) fluorescent cells in alveoli. Bronchoalveolar lavage showed an intense lymphocytic and macrophagic alveolitis (790 cells per mm^3), and foamy macrophages. The dynamic probe-based confocal laser endomicroscopy video sequence is available in the online supplementary material. d: cell diameter. Scale bars=50 µm.

DOI: 10.1183/09031936.00191911

strongly support this hypothesis, but provide evidence that the pCLE observed fluorescent cells do not correspond to this foamy macrophage population.

In contrast to BAL, the accumulation of foamy cells in the lung tissue is believed to be a distinctive histological feature of amiodarone-related pulmonary toxicity [24]. This may suggest that pCLE allows *in situ* observation of activated cells in the interstitial and intra-alveolar lung compartments, whereas BAL reflects the cell populations present in the bronchiolar and alveolar spaces, independently of their activation. Recently, KELLER *et al.* [25] presented data that support this hypothesis, showing that highly fluorescent cells could be observed *in vivo* in the graft from single lung recipients, whereas the original lung was free of cellular infiltration. This is also in accordance with previous findings from the same group showing that, in stable lung graft recipients, activated inflammatory cells are present in BAL [26]. However, while our microspectrometry analysis suggests a different origin of the cellular fluorescent signal in AMR-IP compared with smokers, the demonstration of the cellular or molecular processes underlying the cellular fluorescence requires further fundamental experiments.

One of the limitations of our study is that, as usual in drug-induced lung diseases, classification of the patient relies on probability diagnostic criteria. Here, we used, along with a strict agreement between experts, very stringent criteria for AMR-IP, in which the presence of an alternative cause of ILD classifies the patient as having a low probability of drug-related disease. Therefore, it is possible that some patients with a low probability of AMR-IP might have underlying amiodarone lung toxicity as part, or as a trigger, of the acute lung disease. This may also explain why slightly fluorescent cells could be found in alveolar areas of such patients using pCLE. Conversely, pCLE follow-up might be helpful for early detection of lung toxicity in patients taking amiodarone, and to monitor the regression of the cellular infiltration along with the improvement of the ILD as the responsible drug is discontinued.

As all amiodarone-treated patients included in our study were nonsmokers at the time of alveoscopy, it cannot be excluded that pCLE specificity for AMR-IP may be low in smoking patients. In particular, it is possible that, in smokers, the tobacco tar-induced cell fluorescence masks the fluorescent signal related to the drug toxicity. Therefore, the results presented here only apply to nonsmoking subjects. However, whereas our *in vivo* spectrometric study is still limited and does not include nonsmoking patients not taking amiodarone, it indicates that the fluorescent signal from tobacco tar can be distinguished from that of the AMR-IP. Future studies are needed to confirm the usefulness of *in situ* microspectrometry in smoking patients receiving amiodarone.

In conclusion, pCLE is a minimally invasive technique that can be easily added to a simple endoscopic procedure in the context of possible drug-induced lung disease. The procedure appears particularly valuable in nonsmoking ILD patients taking amiodarone, for whom the discontinuation of the drug may be problematic, and should be rapidly decided. Future prospective studies are needed to confirm our data,

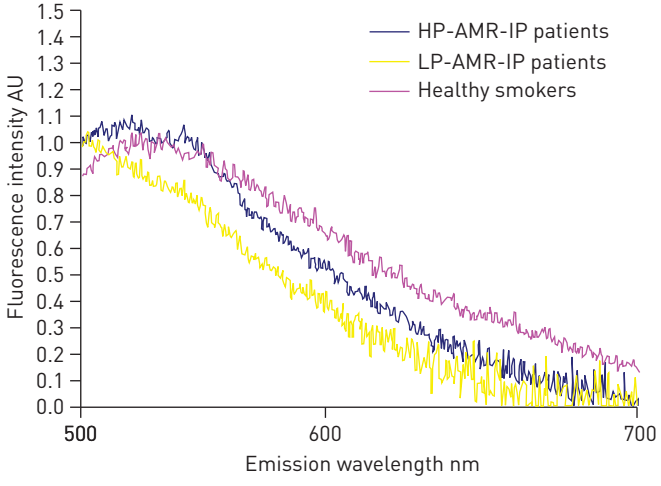

FIGURE 5 *In situ* alveolar microspectrometry in high probability for amiodarone-related interstitial pneumonia (HP-AMR-IP) patients, low probability for amiodarone-related interstitial pneumonia (LP-AMR-IP) patients, and healthy smokers. Each curve represents the mean alveolar autofluorescence spectrum from a group of subjects after excitation at 488 nm. Blue: spectra acquired from non-smoking HP-AMR-IP patients (n=16); yellow: spectra acquired from nonsmoking LP-AMR-IP patients (n=8); and pink: reference spectra from healthy smokers included in our previous study (n=7) [16]. The fluorescence microspectrometry analysis can discriminate the different groups of patients. AU: arbitrary units.

which currently support a decision of drug discontinuation in the presence of alveolar large and highly fluorescent cells during pCLE imaging.

Acknowledgement

The authors wish to thank J-F. Ménard (Medical School – Rouen University, Rouen, France) for his very helpful assistance in biostatistics.

References

1 Connolly SJ. Evidence-based analysis of amiodarone efficacy and safety. *Circulation* 1999; 100: 2025–2034.
2 Vassallo P, Trohman RG. Prescribing amiodarone: an evidence-based review of clinical indications. *JAMA* 2007; 298: 1312–1322.
3 Rakita L, Sobol SM, Mostow N, *et al.* Amiodarone pulmonary toxicity. *Am Heart J* 1983; 106: 906–916.
4 Rotmensch HH, Liron M, Tupilski M, *et al.* Possible association of pneumonitis with amiodarone therapy. *Am Heart J* 1980; 100: 412–413.
5 Ashrafian H, Davey P. Is amiodarone an underrecognized cause of acute respiratory failure in the ICU? *Chest* 2001; 120: 275–282.
6 Brinker A, Johnston M. Acute pulmonary injury in association with amiodarone. *Chest* 2004; 125: 1591–1592.
7 Dusman RE, Stanton MS, Miles WM, *et al.* Clinical features of amiodarone-induced pulmonary toxicity. *Circulation* 1990; 82: 51–59.
8 Greenspon AJ, Kidwell GA, Hurley W, *et al.* Amiodarone-related postoperative adult respiratory distress syndrome. *Circulation* 1991; 84: Suppl., III407–III415.
9 Wood DL, Osborn MJ, Rooke J, *et al.* Amiodarone pulmonary toxicity: report of two cases associated with rapidly progressive fatal adult respiratory distress syndrome after pulmonary angiography. *Mayo Clin Proc* 1985; 60: 601–603.
10 Effect of prophylactic amiodarone on mortality after acute myocardial infarction and in congestive heart failure: meta-analysis of individual data from 6500 patients in randomised trials. Amiodarone trials meta-analysis investigators. *Lancet* 1997; 350: 1417–1424.
11 Singh SN, Fisher SG, Deedwania PC, *et al.* Pulmonary effect of amiodarone in patients with heart failure. The congestive heart failure-survival trial of antiarrhythmic therapy (CHF-STAT) investigators (veterans affairs cooperative study no. 320). *J Am Coll Cardiol* 1997; 30: 514–517.
12 Roca J, Heras M, Rodriguez-Roisin R, *et al.* Pulmonary complications after long term amiodarone treatment. *Thorax* 1992; 47: 372–376.
13 Martin WJ 2nd, Osborn MJ, Douglas WW. Amiodarone pulmonary toxicity. Assessment by bronchoalveolar lavage. *Chest* 1985; 88: 630–631.
14 Bedrossian CW, Warren CJ, Ohar J, *et al.* Amiodarone pulmonary toxicity: cytopathology, ultrastructure, and immunocytochemistry. *Ann Diagn Pathol* 1997; 1: 47–56.
15 Thiberville L, Moreno-Swirc S, Vercauteren T, *et al. In vivo* imaging of the bronchial wall microstructure using fibered confocal fluorescence microscopy. *Am J Respir Crit Care Med* 2007; 175: 22–31.
16 Thiberville L, Salaün M, Lachkar S, *et al.* Human *in vivo* fluorescence microimaging of the alveolar ducts and sacs during bronchoscopy. *Eur Respir J* 2009; 33: 974–985.
17 Thiberville L, Salaün M, Lachkar S, *et al.* Confocal fluorescence endomicroscopy of the human airways. *Proc Am Thorac Soc* 2009; 6: 444–449.
18 Newton R, Kemp S, Zoumot Z, *et al.* An unusual case of haemoptysis. *Thorax* 2010; 65: 309.
19 Mercer RR, Crapo JD. Spatial distribution of collagen and elastin fibers in the lungs. *J Appl Physiol* 1990; 69: 756–765.
20 Weibel ER, Sapoval B, Filoche M. Design of peripheral airways for efficient gas exchange. *Respir Physiol Neurobiol* 2005; 148: 3–21.
21 Désir C, Petitjean C, Heutte L, *et al.* Using *a priori* knowledge to classify *in vivo* images of the lung. *Lect Notes Comp Sci* 2010; 6216: 207–212.
22 Thiberville L, Salaün M, Bourg-Heckly G. *In vivo* confocal microendoscopy: from the proximal bronchus down to the pulmonary acinus. *In:* Strausz J, Bolliger CT, eds. Interventional Pulmonology. *Eur Respir Monogr* 2010; 48: 73–89.
23 Kahn FW, Jones JM, England DM. Diagnosis of pulmonary hemorrhage in the immunocompromised host. *Am Rev Respir Dis* 1987; 136: 155–160.
24 Camus P. Drug-induced infiltrative lung diseases. *In:* Schwarz MI, King T, eds. Infiltrative Lung Diseases. 4th Edn. Hamilton, BC Decker, Inc., 2003; pp. 485–534.
25 Keller CA, Erasmus D, Alvarez F, *et al.* Preliminary observations in the use of confocal alveolar endomicroscopy in recipients of single lung transplantation. *Am J Respir Crit Care Med* 2010; 181: A4316.
26 Trello CA, Williams DA, Keller CA, *et al.* Increased gelatinolytic activity in bronchoalveolar lavage fluid in stable lung transplant recipients. *Am J Respir Crit Care Med* 1997; 156: 1978–1986.

DOI: 10.1183/09031936.00191911